Polymer Chain Extension in Semibatch Emulsion Polymerization with RAFT-Based Transfer Agent: The Influence of Reaction Conditions on Polymerization Rate and Product Properties

Ibrahem S. Altarawneh, Vincent G. Gomes, Mourtada H. Srour

School of Chemical and Biomolecular Engineering, University of Sydney, New South Wales 2006, Australia

Received 18 December 2007; accepted 31 July 2008
DOI 10.1002/app.30752
Published online 7 July 2009 in Wiley InterScience (www.interscience.wiley.com).

ABSTRACT: A mathematical model was developed for batch and semiemulsion polymerizations of styrene in the presence of a xanthate-based RAFT agent. Zero–one kinetics was employed along with population balance equations to predict monomer conversion, molecular weight (MWD), and particle size (PSD) distributions in the presence of xanthate-based RAFT agents. The effects of the transfer agent (AR), surfactant, initiator, and temperature were investigated. Monomer conversion, MWD, and PSD were found to be strongly affected by monomer feed rate. The polymerization rate (Rp), number average molecular weight (Mn) and particle size (r) decreased with increasing AR. With increases in surfactant and initiator concentrations Rp increased, whereas with increase in temperature Mn decreased, Rp increased and r increased. In semibatch mode, Mn and r increased with increase in monomer flow rate. By feeding the RAFT agent along with the monomer ($F_M/F_{AR} = N_{Mo}/N_{ARo} = 100$), Mn attained a constant value proportional to monomer/RAFT molar ratio. The observed retardation in polymerization and growth rates is due to the exit and re-entry of small radicals. Thus, chain extension was successfully achieved in semibatch mode. The simulations compared well with our experimental data, and the model was able to accurately predict monomer conversion, Mn, MWD, and PSD of polymer products. Our simulations and experimental results show that monomer feed rate is suitable for controlling the PSD, and the initial concentration and the feed rate of AR for controlling the MWD and PSD. J Appl Polym Sci 114: 2356–2372, 2009

Key words: semi-batch emulsion polymerization; mathematical model; RAFT; molecular weight distribution; particle size distribution; secondary nucleation styrene; xanthate

INTRODUCTION

Emulsion polymerization is one the most versatile process for manufacturing synthetic polymers with products ranging from elastomeric lattices for coatings, bulk plastics, paints, adhesives to resins. Semibatch emulsion polymerization processes are being used widely for the production of varieties of bulk commodities and value-added products. The process is preferred due to its substantial technical, commercial, and environmental benefits. The reaction medium (water) offers a safe process with high yield and due to low viscosity facilitates overcoming heat, mass, and fluid transport limitations. The process enables control of polymer molecular weight (MWD) and particle size distributions (PSD), which strongly affect product mechanical, rheological, thermal, and chemical properties. MWD is usually controlled by chain transfer agents such as mercaptans[1,2] or living free radical polymerization,[3–5] whereas PSD is controlled by surfactants and optimal process conditions.[6,7]

Living free radical polymerization (LFRP) is a relatively recent development gaining popularity for synthesizing well-defined polymers. LFRP techniques have also been extended to heterogeneous polymerizations such as emulsion and suspension polymerization.[8–12] LFRP with heterogeneous polymerization is an active research area as it provides a powerful tool for preparing tailor-made products and promises substantial practical applications. Three major LFRP techniques are nitroxide-mediated polymerization (NMP),[5] atom transfer radical polymerization (ATRP),[3] and reversible addition-fragmentation chain transfer (RAFT).[4]

RAFT process, due to its flexibility and the use of mild conditions, is the most promising among LFRP for industrial applications. Among others, a key disadvantage of RAFT solution and bulk polymerization is their slow polymerization rates, since radical concentration must be maintained at a low level to minimize radical–radical termination.[4,13] This

Correspondence to: V. G. Gomes (v.gomes@usyd.edu.au).

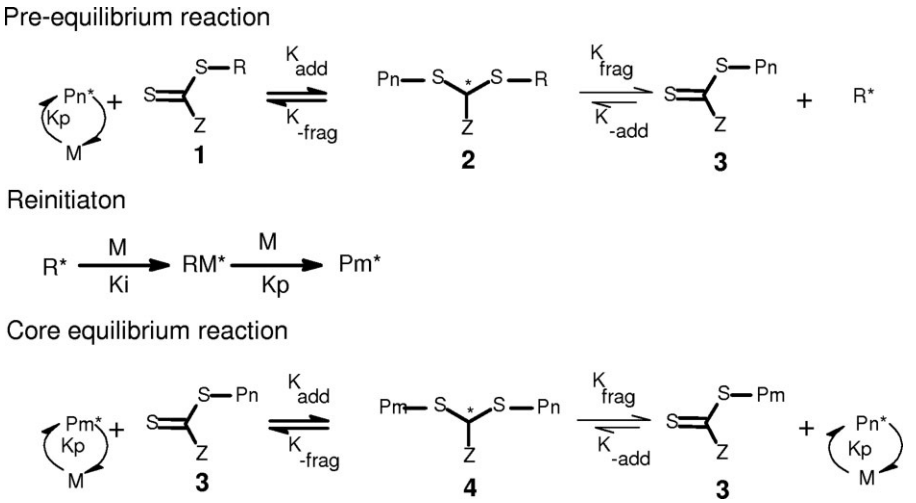

Scheme 1 RAFT mechanism.

problem can be overcome in principle by using emulsion polymerization by taking advantage of radical segregation to decrease termination without significantly reducing the polymerization rate. Hence, combining RAFT with emulsion polymerization has potential in manufacturing polymers such that polymer properties (MWD and PSD) can be controlled precisely.[8,14]

RAFT LFRP is facilitated by compounds having structures such as Z—C(=S)S—R (compound 1 in Scheme 1).[4,15] Such reagents can be designed for structural variety for the "leaving group R" and the "stabilizing group Z." The RAFT polymerization mechanism, as illustrated in Scheme 1, has been well accepted. A polymerization reaction employing RAFT agent is expected to proceed according to the kinetic events given in Scheme 1. The RAFT process (pre and core-equilibriums) is a reversible transfer process in which free radicals exchange degeneratively with dormant species. During the pre-equilibrium stage, addition of the propagating radical **Pn*** to the thiocarbonylthio reagent (compound **1)** followed by forward fragmentation of the carbon-centered intermediate radical (compound **2)**, gives rise to a polymeric RAFT agent (compound **3)** and a new reinitiating radical ***R****. A reaction of the reinitiating radical ***R**** with monomer forms a new propagating radical **Pm*** which adds to the polymeric RAFT agent **3** resulting in a symmetrical carbon-centered intermediate radical **4.** Because the intermediate radical is unstable, it either produces the original chains (backward fragmentation), or results in the exchange of RAFT group between two chains (forward fragmentation).

Despite its successful application with solution and bulk techniques, RAFT polymerization suffers serious problems in emulsion. Lack of colloidal stability, phase separation, rate retardation, and poor molecular weight control especially when a high active RAFT agent (with Ctr>>1) is used have been reported.[14–19] Therefore, successful RAFT LFRP in emulsion requires that the transfer agent distributes itself among the monomer droplets, the aqueous phase, and micelles, and be transported from the droplets through the aqueous phase to the particles. Difficulties in transporting RAFT agent into polymer particles were overcome by use of low active RAFT agents such as xanthates,[8,16,17,20] or by interventions, e.g., using cyclodextrins[21] or water soluble monomers to produce short stabilizing RAFT agents.[22]

In one study,[19] RAFT emulsion polymerization was facilitated by using an organic cosolvent, acetone, to transport the RAFT agent into emulsion seed before polymerization. However, this technique poses safety and environmental problems along with cost and operational drawbacks. Moad et al.,[23] overcame the problem of phase separation by using semibatch process with surfactant (sodium dodecyl sulfate, SDS) and water soluble initiator (potassium persulfate, KPS) in the presence of small amounts of monomer, polymerized at 80°C for 40 min, after which the monomer was fed gradually. With this approach, polymerization during the initial stage occurred in the absence of monomer droplets, resulting in good control of MWD.

Low active RAFT agents such as xanthates are suitable for integration with the classical *ab initio* emulsion polymerization and MADIX or "macromolecular design via the interchange of xanthates."[8,16,17,20] Since most of the polymeric chains carry RAFT moiety, block copolymers are feasible.[24,25] Charmot et al.[16] used *o*-ethylxanthyl ethyl propionate in semibatch emulsion polymerization of *n*-butyl acrylate. A linear growth of Mn and a PDI of 1.4 was reported with no change in polymerization rate and particle size compared with base

case—indicating that radical exit had no effect on the kinetics. Rate retardation was observed by Monteiro and de Barbeyrac[17] in styrene *ab initio* emulsion polymerization with xanthates. They found that the average particle size decreased, and the PSD became narrower with increased concentration of SDS or RAFT agent. Since the chain transfer constant is low, the number average molecular weight (Mn) remained almost constant during polymerization with a constant polydispersity (PDI) of about 2.20. Using a fluorinated xanthate agent, similar effects were reported[15] with a linear growth of Mn and a low PDI ($\sim$ 1.5).

Smulders et al.[20] reported a surprising reduction in entry rate coefficient when *o*-ethylxanthyl ethyl propionate was used in seeded emulsion polymerization of styrene. The authors attributed this to the surface activity of the xanthate molecules. Since the entered z-mers are also surface active, they have a high probability of transfer to RAFT agent, resulting in possible exit instead of propagation. Hence, exit of the radical at the surface results in a decrease in the effective rate of entry. Most kinetic studies have focused on batch heterogeneous polymerizations with various RAFT agents.[11,26–29] However, a comprehensive model for RAFT process in batch and semibatch emulsion polymerization is lacking. Thus, the operational and differential aspects with batch and semibatch RAFT processes still remain unexplored. Modelling of RAFT emulsion polymerization to accurately predict polymer architectural properties (MWD and PSD) is of great practical significance as it is crucial in design, scale-up, and developing desirable new products for the market.

It is reasonable that living polymerization could be approached with a low active RAFT agent if the rate of transfer over the rate of propagation is increased via controlled feed rate of monomer.[20] Thus, this work aims to address the application of low active RAFT-based transfer agent (xanthate) in semibatch emulsion polymerization of styrene with controlled monomer feed. For precise control of product properties and process understanding, we developed a dynamic model for RAFT emulsion polymerization[8] combining conventional emulsion polymerization kinetics[6,7,30] with RAFT process kinetics.[4,11,20,27,31]

MODELLING RAFT EMULSION POLYMERIZATION

Our RAFT emulsion polymerization model accounts for reactions in the aqueous and particle phases during propagation, termination, transfer to monomer and RAFT exchange, along with radical absorption and desorption to and from particles. The details of the model and parameters are available elsewhere.[8] Here, we outline the essential elements for understanding the results.

A "zero-one" model (reasonable for emulsion systems) is based on the premise that the rate of radical–radical bimolecular termination within a latex particle is fast relative to the rate of radical entry into particles. Thus, a particle has either zero or one radical. Theory[32] and experiments[33] confirm that the zero–one mechanism is valid when the particles are small ($\sim$ 100 nm) and are saturated with monomer such that glassy transition is not reached. Polymerization within a relatively large particle is governed by pseudo-bulk kinetics. The size at which particles cross from the zero–one to the pseudo-bulk regime varies from monomer to monomer, and is known as the "cross-over radius." The cross-over diameter for styrene was reported to be 100–120 nm.[6,34,35] Small particle size corresponds to lower radical entry rate, higher radical exit, and higher termination rates.[6] Our experiments were designed to produce latex particles with a maximum average diameter of 100 nm.

Aqueous phase mass balance

The process begins with the formation of radicals (from the initiator), which then react with monomers to form oligomeric radicals. These radicals ($P_n^{\bullet}$) may propagate, add to the AR and terminate with another radical. Entry into a micelle or an existing particle occurs only when the oligomeric radical attains a degree of polymerization greater than or equal to the critical degree of polymerization "z," when the oligomer becomes surface active. The model is used to determine the number of styrene units that an oligomer must have (z) to reduce its solubility and hence impart surface activity for entry to a particle or micelle. To impart surface activity, the minimum hydrophobic free energy required is $\Delta G^{\mathrm{hyd}} \approx 23{,}000$ J mol^{-1}. On the basis of this, excellent agreement[6,35] was obtained experimentally for styrene/persulfate systems with $z = 3$. Particle formation occurs either by entry of the aqueous phase z-mers into micelle if micelles are present in the system or by collapsing if their degree of polymerization is above a critical degree of polymerization for homogenous nucleation ($j_{\mathrm{crit}} = 5$).

In the aqueous phase, addition of RAFT agent results in an unstable intermediate radical. The fragmentation of the intermediate radical generates a dormant species a carrying RAFT moiety and acts as a new propagating radical (leaving-group radical). Since the rate of fragmentation is relatively faster than that of addition,[8,36] the RAFT reaction in the aqueous phase is approximated as a transfer reaction of the RAFT group (R) without affecting the overall radical concentration in the aqueous phase. The leaving-

group radical (RAFT-derived R^*) may enter a micelle or an existing particle when it has sufficient surface activity. R^* has the same fate as the initiator derived radical in the aqueous phase and displays similar behaviour in propagation, entry and termination.

The propagating polymeric radical in the particle may undergo a radical transfer reaction with a monomer molecule, producing the monomeric radical ($M^\bullet$) and with RAFT agent producing a RAFT-derived radical ($R^\bullet$).[36] If it escapes termination, such radicals may convert into less water-soluble ones that cannot exit the particle. However, these radicals (($R^\bullet$) and ($M^\bullet$)) may also diffuse through the interior of the latex particle to the particle surface where they can exit the particle as exited radicals, $E^\bullet$.[6] Once the desorbed monomeric radical or RAFT-derived radical meets the surface of a particle, it immediately penetrates the particle due to its high lipophilic nature, and the aqueous phase propagation/termination are insignificant for the desorbed radicals.[30,37] The sorption/desorption process is reversible:

$$E^* + \text{Particle} \quad \underset{k_{dE}}{\overset{k_{eE}}{\rightleftharpoons}} \quad \text{particle} - E^*$$

For the reactions in the aqueous phase, mass balance equations were set up, whereas for the particle phase, Smith-Ewart PBEs were modified,[8] to account for the application of RAFT agent. Mass balances of the various aqueous species are given by:

$$\frac{d[I]}{dt} = -k_d[I] \tag{1}$$

$$\frac{d[I^\bullet]}{dt} = 2fk_d[I] - k^1_{\text{p,aq}}[I^\bullet]C^M_w \tag{2}$$

$$\frac{d[P^\bullet_1]}{dt} = k^1_{\text{p,aq}}[I^\bullet]C^M_w - k^1_{\text{p,aq}}[P^\bullet_1]C^M_w - k^{\text{AR}}_{\text{tr,aq}}[P^\bullet_1]C^{\text{AR}}_w - k_{\text{t,aq}}[P^\bullet_1][T^\bullet_{\text{aq}}] \tag{3}$$

For $n < z$ then

$$\frac{d[P^\bullet_n]}{dt} = k^{n-1}_{\text{p,aq}}[P^\bullet_{n-1}]C^M_w - k^n_{\text{p,aq}}[P^\bullet_n]C^M_w - k^{\text{AR}}_{\text{tr,aq}}[P^\bullet_n]C^{\text{AR}}_w - k_{\text{t,aq}}[P^\bullet_n][T^\bullet_{\text{aq}}] \tag{4}$$

For $n = z,\ldots,j_{\text{crit}} - 1$ then

$$\frac{d[P^\bullet_n]}{dt} = k^{n-1}_{\text{p,aq}}[P^\bullet_{n-1}]C^M_w - k^n_{\text{p,aq}}[P^\bullet_n]C^M_w - k^{\text{AR}}_{\text{tr,aq}}[P^\bullet_n]C^{\text{AR}}_w - k_{\text{t,aq}}[P^\bullet_n][T^\bullet_{\text{aq}}] - k^i_e[P^\bullet_n]\frac{N_{\text{tot}}}{N_A} - k^i_{e,\text{micelle}}C_{\text{micelle}}[P^\bullet_n] \tag{5}$$

$$\frac{d[P^\bullet_{j_{\text{crit}}}]}{dt} = k^{j_{\text{crit}}-1}_{\text{p,aq}}[P^\bullet_{j_{\text{crit}}-1}]C^M_w - k_{\text{t,aq}}[P^\bullet_{j_{\text{crit}}}][T^\bullet_{\text{aq}}] \tag{6}$$

$$\frac{d[E^\bullet]}{dt} = \sum_{n=1}^{j_{\text{crit}}-1} k^{\text{AR}}_{\text{tr}}[P^\bullet_n]C^{\text{AR}}_w - k^E_e[E^\bullet]\frac{N_{\text{tot}}}{N_A} - k^R_{e,\text{micelle}}C_{\text{micelle}}[E^\bullet] + k^E_d\frac{N^R_1}{N_A} - k_{\text{t,aq}}[E^\bullet][T^\bullet_{\text{aq}}] \tag{7}$$

$$[T^\bullet_{\text{aq}}] = [E^\bullet] + \sum_{i=1}^{z-1}[P^\bullet_n] \tag{8}$$

C^M_w and C^{AR}_w are the concentrations of monomer and RAFT agent in the aqueous phase respectively; N_{tot} is the total number of latex particle per liter of aqueous phase, and N_A is Avogadro's number. N^R_l is the number concentration particles with one RAFT-derived radical or monomeric radical per litre of aqueous phase. $P^\bullet_n$, $R^\bullet_{\text{aq}}$ are the concentrations of oligomeric initiator-derived radical and RAFT-derived radical in the aqueous phase, respectively; k^i_e, $k^i_{e,\text{micelle}}$, k^R_e, $k^R_{e,\text{micelle}}$ are the second order entry rate coefficients of the initiator and RAFT-derived radicals into a particle, and a micelle, respectively; k_{dE} is the rate coefficient for desorption of monomeric and RAFT radicals into the water phase; $K^{\text{AR}}_{\text{tr,aq}}$ is the transfer rate coefficient of the aqueous phase radicals to RAFT agent.

The concentration of the aqueous phase radicals T^*_{aq} is given by the summation of RAFT-derived radical generated in the aqueous phase, aqueous phase oligomeric radical P^*_{aq} and exited radicals. The aqueous phase propagation and termination rate coefficients are characterized by "$k^i_{\text{p,aq}}$" and "$k_{\text{t,aq}}$," respectively; f is the initiator efficiency and is simultaneously calculated by solving the aqueous phase rate equations (eqs. (1)–(8)). Equation (2) takes into account the fact that the propagation of an initiator fragment with a monomer is so fast as not to be rate determining step.[30,37] While eqs. (3)–(5) account for RAFT reactions with monomer in the aqueous phase.[8,20]

Micellar concentration (C_{micelle}) was determined from the rate of surfactant consumption and the maximising function[7]:

$$C_{\text{micelle}} = \text{Maximum}\left[0, \frac{[S_{\text{added}}] - [S_{\text{ads}}] - [\text{cmc}]}{n_{\text{agg}}}\right] \tag{9}$$

$$S_{\text{ads}} = \frac{4\pi}{N_A a_s}\int_0^\infty r_s^2 n(r)dr \approx \frac{4\pi r_s^2 N_{\text{tot}}}{N_A a_s} \tag{10}$$

where cmc is the critical micellar concentration; n_{agg} is the mean aggregation number for the surfactant; S_{added} is the total concentration of the added surfactant; S_{ads} represents the amount of surfactant per unit volume adsorbed onto the polymer surface; a_s is the area occupied by an adsorbed surfactant molecule. From eq. (9) one can conclude that micellar nucleation (particle formation via micelles) stops

when the surfactant concentration falls below its critical value (cmc).

Particle phase balance equations

Population balance equations are conveniently expressed in terms of unswollen volume (V). The equations can also be expressed in terms of unswollen radius (r), and the two distribution functions are related via:

$$n(V) = n(r)/4\pi r^2$$

where, radius and volume distributions are denoted by $n(r)$ and $n(V)$, respectively. The simplest version of zero-one model for RAFT-free systems accounts only for the number of particles with one radical and without any radicals. Differently from this approach, in the presence of RAFT agent the particles are distinguished in this work upon the type of radical that they contain. These particles are:

1. Particles containing no free radicals (n_0) generated by entry of a radical into (n_1^R) and (n_1^P) type radicals. They are also formed when monomeric and RAFT derived radicals exit an (n_1^R) type particle. The population of (n_0) decreases when oligomeric (P_n^*) and small exited (E^*) radicals enter an existing (n_0) type particle:

$$\frac{\partial n_0(V,t)}{\partial t} = \rho(n_1^P + n_1^{\mathrm{PAR}} + n_1^{\mathrm{PAP}} + n_1^{\mathrm{RAR}} + n_1^{\mathrm{RAP}} + n_1^R - n_0) + k_{dE} \times n_1^R \quad (11)$$

2. Particles containing a monomeric or a RAFT-derived radical (n_1^R) generated by entry of small radical (monomeric or RAFT derived radical) into (n_0) type particle, transfer reaction to RAFT agent or to monomer within (n_1^R) and (n_1^P) type particles and by the fragmentation of the intermediate radical in (n_1^{PAR}), (n_1^{RAR}) and (n_1^{RAP}) type particles. The population of (n_1^R) decreases by propagation, entry of any radical into such type of particle, exit, transfer to monomer and by exchange with RAFT agent:

$$\frac{\partial n_1^R(V,t)}{\partial t} = k^R_{e,\mathrm{micelle}} C_{\mathrm{micelle}}[E] + k_{eE}[E]n_0 - \rho n_1^R - k_{dE} n_1^R - k_p^R C_p^M n_1^R - k_{\mathrm{add}} C_P^{\mathrm{AR}} n_1^R - k_{\mathrm{add}} C_P^{\mathrm{AP}} n_1^R + k^{\mathrm{RAP}}_{-\mathrm{frag}} \times n_1^{\mathrm{RAP}} + k^{\mathrm{PAR}}_{\mathrm{frag}} \times n_1^{\mathrm{PAR}} + k^{\mathrm{RAR}}_{\mathrm{frag}} \times n_1^{\mathrm{RAR}} + k^{\mathrm{RAR}}_{-\mathrm{frag}} \times n_1^{\mathrm{RAR}} + k_{\mathrm{tr}}^M C_p^M n_1^P \quad (12)$$

3. Particles containing a single polymeric radical (n_1^P), generated by the entry of an initiator derived radical (P_n^*) with degree of polymerization equal or greater than three ($n \geq z$) into a zero radical particle (n_0), propagation of a small radical within an (n_1^R), and by fragmentation of the intermediate radical within (n_1^{PAR}), (n_1^{PAP}) and (n_1^{RAP}) type particles. Particles containing such polymeric radical are consumed by entry of any radical from the aqueous phase into this type of particles resulting in instantaneous termination, by transfer to monomer and by exchange with RAFT agent. Propagation within this kind of particles does not change their identity:

$$\frac{\partial n_1^P(V,t)}{\partial t} = \delta(V - V_o)\left[k^{J_{\mathrm{crit}}-1}_{\mathrm{p,aq}} C_w^M [P^\bullet_{J_{\mathrm{crit}}-1}] + \sum_{n=1}^{J_{\mathrm{crit}}-1} k^i_{e,\mathrm{micelle}} C_{\mathrm{micelle}}[P_n^\bullet]\right] + k_p^R C_p^M n_1^R - k_{\mathrm{add}} C_P^{\mathrm{AR}} n_1^P - k_{\mathrm{add}} C_P^{\mathrm{AP}} n_1^P + k^{\mathrm{PAR}}_{-\mathrm{frag}} \times n_1^{\mathrm{PAR}} + k^{\mathrm{RAP}}_{\mathrm{frag}} \times n_1^{\mathrm{RAP}} + k^{\mathrm{PAP}}_{\mathrm{frag}} \times n_1^{\mathrm{PAP}} + k^{\mathrm{PAP}}_{-\mathrm{frag}} \times n_1^{\mathrm{PAP}} - k_{\mathrm{tr}}^M C_p^M n_1^P + \rho_i n_0 - \rho n_1^P - \frac{\partial (K n_1^P)}{\partial V} \quad (13)$$

where K is the propagational growth rate for particle containing a single free radical and is given by[6,7,30,35]:

$$K(V) = k_p M_w^M C_p(V)/N_A d_p \quad (14)$$

where $C_p(V)$ is monomer concentration in the particle as a function of particle size; d_p is polymer density; M_w^M is the molecular weight of the monomer. Growth significantly affects n_1^{PAR} type particles only, as radicals propagate without changing particle identity.

4. Particles containing an intermediate radical (n_1^{PAR}), generated from the addition of a polymeric radical to the RAFT agent (AR):

$$\frac{\partial n_1^{\mathrm{PAR}}(V,t)}{\partial t} = k_{\mathrm{add}} C_p^{\mathrm{AR}} n_1^P - (k_{\mathrm{frag}} + k_{-\mathrm{frag}}) n_1^{\mathrm{PAR}} - \rho n_1^{\mathrm{PAR}} \quad (15)$$

5. Particles containing an intermediate radical (n_1^{PAP}) generated from the addition of a polymeric radical (P_n^*) to the polymeric RAFT agent (AP).

$$\frac{\partial n_1^{PAP}(V,t)}{\partial t} = k_{\mathrm{add}} C_p^{\mathrm{AP}} n_1^P - (k_{\mathrm{frag}} + k_{-\mathrm{frag}}) n_1^{\mathrm{PAP}} - \rho n_1^{\mathrm{PAP}} \quad (16)$$

6. Particles containing an intermediate radical n_1^{RAR} generated from the addition of a small radical to the RAFT agent (AR).

$$\frac{\partial n_1^{\mathrm{RAR}}(V,t)}{\partial t} = k_{\mathrm{add}} C_p^{\mathrm{AR}} n_1^R - (k_{\mathrm{frag}} + k_{-\mathrm{frag}}) n_1^{\mathrm{RAR}} - \rho n_1^{\mathrm{RAR}]} \quad (17)$$

7. Particles containing an intermediate radical generated from the addition of a small radical to the polymeric RAFT agent (AP) (n_1^{RAP}).

$$\frac{\partial n_1^{\mathrm{RAP}}(V,t)}{\partial t} = k_{\mathrm{add}} C_p^{\mathrm{AP}} n_1^R - (k_{\mathrm{frag}} + k_{-\mathrm{frag}}) n_1^{\mathrm{RAP}} - \rho n_1^{\mathrm{RAP}} \quad (18)$$

The cross termination between an intermediate and propagating radical was experimentally confirmed,[38] and such particles are consumed on entry to a aqueous phase radical. The polymer volume fraction inside the particle, an indicator of the particle state, is given by:

$$\Phi_P = 1 - (C_P M_w^M / d_m) \quad (19)$$

Equation (13) accounts for particle formation by both micellar and homogenous mechanisms, through the terms involving $k^i_{e,\mathrm{micelle}} C_{\mathrm{micelle}} [P^\bullet_{\mathrm{n}}]$ for micellar nucleation via radical entry into a micelle to form a precursor particle and $k^{J_{\mathrm{crit}}-1}_{p,\mathrm{aq}} C_w^M [P^\bullet_{J_{\mathrm{crit}}-1}]$ for homogenous nucleation.

Monomer and RAFT concentrations

Our experimental data show that styrene emulsion polymerization is unaffected by monomer diffusional limitation as mass transfer rate is high.[2] Thus, a model with constant partition coefficients in combination with overall mass balances can be built to compute monomer concentration.[2,7,8,39,40] Further, RAFT agent consumption rate was found to be lower than its transport rate from the droplets to particles. Hence, RAFT mass transfer is not a rate determining step for the three phases in emulsion polymerization: water (w), monomer droplets (d) and polymer particles (p). The monomer partition coefficients were calculated from saturation data of the monomer in water and polymer particle:

$$K^i_{wp} = C_{w,\mathrm{sat}}{}^i / C^i_{p,\mathrm{sat}}$$

$$K^i_{\mathrm{dp}} = d_i K^i_{\mathrm{wp}} / M^i_w C^i_{W\mathrm{sat}}, \qquad K^i_{\mathrm{dw}} = K^i_{\mathrm{dp}} / K^i_{\mathrm{wp}} \quad (20)$$

where K^i_{wp}, k^i_{dp}, K^i_{dw} are the partition coefficient of species i between water-particle, droplet-particle and droplet-water phases, respectively. C^i_p, C^i_w, C^i_d are the concentrations of species i in the particle, water and droplet phases, respectively. The volumes of droplet (V_d), water (V_w), and particle (V_p) phases are given as follows:

$$V_d = (N_m M_w^M + N_{\mathrm{AR}} M_w^{\mathrm{AR}} - C_w^M M_w^M V_w - C_w^{\mathrm{AR}} M_w^{\mathrm{AR}} V_w - C_p^M M_w^M V_p - C_p^{\mathrm{AR}} M_w^{\mathrm{AR}} V_p)/d_m \quad (21)$$

$$V_w = V_{\mathrm{wo}} / (1 - ((M_w^M C_w^M / d_m) + (M_w^{\mathrm{AR}} C_w^{\mathrm{AR}} / d_{\mathrm{raft}})) \quad (22)$$

$$\frac{dV_p}{dt} = M_w^M R_p^M V_r / d_p \quad (23)$$

The total reaction volume (V_r) is:

$$\frac{dV_r}{dt} = M_w^M R_p^M V_r (1/d_p - 1/d_m) + M_w^{\mathrm{AR}} R_p^{\mathrm{AR}} V_r (1/d_p - 1/d_{\mathrm{AR}}) + F_m M_w^M / d_m + F_{\mathrm{AR}} M_w^{\mathrm{AR}} / d_{\mathrm{AR}} \quad (24)$$

F_m, F_{AR} are the monomer and RAFT agent feed rates, respectively; M_w^M, M_w^{AR} are the molecular weight of the monomer and RAFT agent, respectively. The polymerization rate (R_p^M) and the consumption rate of the RAFT agent (R_p^{AR}) are given as follows:

$$R_p^M = k_p C_p^M C_p^{\mathrm{Rad}} \quad (25)$$

$$R_p^{\mathrm{AR}} = k_{\mathrm{add}} C_p^{\mathrm{AR}} C_p^{\mathrm{Rad}} - k_{-\mathrm{frag}}^{\mathrm{PAR}} C_p^{\mathrm{PAR}} - k_{\mathrm{frag}}^{\mathrm{RAP}} C_p^{\mathrm{RAP}} - (k_{\mathrm{frag}}^{\mathrm{RAR}} + k_{-\mathrm{frag}}^{\mathrm{RAR}}) C_p^{\mathrm{RAR}} \quad (26)$$

C_p^{Rad} is the concentration of radicals inside particle: $C_p^{\mathrm{Rad}} = \overline{n}(N_{\mathrm{tot}}/N_{\mathrm{A}})(V_w/V_r)$; ($C_p^{\mathrm{RAR}}$, C_p^{RAP}, C_p^{PAR}) are concentrations of intermediate radicals RAR, RAP, and PAR in the particle, respectively. Inside the particle, each addition of a propagating radical to the RAFT agent (AR) results in a new radical and polymeric RAFT agent (AP). Hence, the production rate of the polymeric RAFT agent (AP) is equal to the consumption rate of the RAFT agent (AR). Mass balances for the monomer and the RAFT agent in the three phases are:

$$\frac{dN_m}{dt} = F_m - R_p^M V_r \quad (27)$$

$$\frac{dN_{\mathrm{AR}}}{dt} = F_{\mathrm{AR}} - R_p^{\mathrm{AR}} V_r \quad (28)$$

$$\frac{dN_{\mathrm{AP}}}{dt} = R_p^{\mathrm{AR}} V_r \quad (29)$$

$$C_p^M = \left(\frac{N_m}{V_p + K_{\mathrm{wp}}^M V_w + K_{\mathrm{dp}}^M V_d} \right) \quad (30)$$

$$C_p^{\mathrm{AR}} = \left(\frac{N_{\mathrm{AR}}}{V_p + K_{\mathrm{wp}}^{\mathrm{AR}} V_w + K_{\mathrm{dp}}^{\mathrm{AR}} V_d} \right) \quad (31)$$

$$C_p^{AP} = \left(\frac{N_{AP}}{V_p}\right) \quad (32)$$

(C_p^{AP}) is the concentration of dormant polymeric chains in a particle; (N_{AP}), the moles of dormant polymeric RAFT agent, is equal to the reacted moles of initial AR.

Kinetic parameters

The entry of radicals from an initiator occurs only for radicals of degree of polymerization "z" or greater, while entry and re-entry of R^* and an exited radical does not require such a condition. The entry of a z-mer into a particle and micelle, and hence their rate coefficients k_e^i and $k_{e,\text{micelle}}^i$, are size dependent and diffusion-controlled with an exponent of ½, characterizing its chain length-dependent coefficient.[6,7,30] The entry rate coefficients for the z-mer and R*, estimated from the Smoluchowski equation are given as follows:

- Entry rate coefficient of z-mer to the particles:

$$k_e^i(V) = 4\pi r_s N_A \frac{D_w}{i^{1/2}}, \quad i \geq z; \qquad k_e^i(V) = 0.0, \quad i < z \quad (33)$$

- Entry rate coefficient of z-mer to the micelles:

$$k_{e,\text{micelle}}^i(V) = 4\pi r_{\text{micelle}} N_A \frac{D_w}{i^{1/2}}, \quad i \geq z; \qquad k_{e,\text{micelle}}^i(V) = 0.0, \quad i < z \quad (34)$$

- Entry rate coefficient of R* to the particles:

$$k_e^R(V) = 4\pi r_s N_A D_R \quad (35)$$

- Entry rate coefficient of R* to the micelles:

$$k_{e,\text{micelle}}^R(V) = 4\pi r_{\text{micelle}} N_A D_R \quad (36)$$

where D_R and D_w are diffusion coefficients of R^* and M* in water phase; r_{micelle}, r_s are radii of micelles and latex particles swollen with monomer. The rate of diffusion of the RAFT radical is similar to that for the monomeric radical. As the RAFT-derived radical is surface-active and water insoluble, it is considered that the exited radicals re-enter without propagating, i.e., its degree of polymerization is 1.[32] The re-entry rate coefficient for exited small radical (E^*) is defined similarly:

$$k_e^M(V) = k_e^R(V) = keE(V) = 4\pi r_s N_A D_w \quad (37)$$

The rate coefficient for desorption of small radicals (E^*) is a function of radical diffusion in water and particle, the aqueous and particle concentrations of the desorbed radical, and the particle volume. For monomeric radicals the coefficient is given by:

$$k_{dE}(V) = \frac{3D_w D_{\text{mon}}}{(qD_{\text{mon}} + D_w)r_s^2} \quad (38)$$

where q, the partition coefficient of exited monomeric species, is equal to C_P/C_w; D_{mon}, the diffusion coefficient for the monomer inside the particle, is given by the following equations:

$$D_{\text{mon}} = 10^{0.417\phi - 29.51\Phi_p + 53.14\Phi_p^2 - 36.03\Phi_p^3}, \text{ for } \Phi_p < 0.8$$

$$D_{\text{mon}} = 9^* 10^{-8} \exp(-19.16\Phi_p), \text{ for } \Phi_p \geq 0.8 \quad (39)$$

where Φ_p is the polymer volume fraction inside the particle. At high Φ_p the particle becomes glassy, resulting in reduced entry rate of z-mer into a particle and is accounted by entry efficiency: $\varepsilon = (1 - \Phi_p)^{C_{P,\text{satt}}^M}$.[7] The overall entry rate (ρ) is given by:

$$\rho = k_{eE}[E] + \sum_{i=z}^{i=j_{\text{crit}}-1} k_e^i[IM_i] \quad (40)$$

Accurate propagation rate coefficient was obtained from pulsed laser polymerization[41] in conjunction with MWD data for styrene: $k_{\text{po}} = 10^{7.63} \exp(-32500/RT)$. At high monomer conversion when the viscosity in the particle increases sharply, the propagation and termination rates become diffusion controlled, and the zero-one kinetics no longer holds. This is incorporated via:

$$k_p = 1/(1/k_{\text{po}} + 1/k_{\text{diff}}) \quad (41)$$

where k_{po} is the propagation rate coefficient at low conversion, while k_{diff} is the diffusion controlled rate coefficient given by $k_{\text{diff}} = 4\pi\sigma N_A(D_{\text{mon}} + D_{\text{rd}})$, ($D_{\text{rd}} = k_p C_p \alpha^2/6$). Similarly, the termination rate coefficient is estimated from[7]:

$$k_t = k_{\text{to}} \exp(-19\Phi_p^{2.1}) \quad (42)$$

where k_{to} is termination rate coefficient at low conversion.

The overall transfer rate coefficient (k_{tr}^{AR}) is represented by a composite of addition-fragmentation rate coefficients, and from the pre or core-equilibrium reactions (Scheme 1), the backward ($k_{-\text{tr}}^{AR}$) and forward (k_{tr}^{AR}) transfer rate coefficients are given by:

$$k_{\text{tr}}^{AR} = k_{\text{add}} \frac{k_{\text{frag}}}{k_{\text{frag}} + k_{-\text{frag}}} \quad (43)$$

$$k_{-\mathrm{tr}}^{\mathrm{AR}} = k_{-\mathrm{add}} \frac{k_{-\mathrm{frag}}}{k_{\mathrm{frag}} + k_{-\mathrm{frag}}} \tag{44}$$

The transfer constant is defined as the ratio of the transfer rate coefficient ($k_{\mathrm{tr}}^{\mathrm{AR}}$) and the propagation rate coefficient (k_p):

$$C_{\mathrm{tr}} = \frac{k_{\mathrm{tr}}}{k_p} \tag{45}$$

Our RAFT agent has a transfer rate constant of 0.7.[20,42] In the pre-equilibrium stage, larger chains are most likely to be released resulting in shift of equilibrium toward the starting materials. Thus, the backward fragmentation rate coefficient of the intermediate radical of type PAR is greater than the forward fragmentation rate coefficient. As the concentration of small radicals from the fragmentation of the intermediate radical is relatively negligible, the backward addition is insignificant. Considering symmetrical intermediate radicals (core-equilibrium stage), the addition rate is ($k_{\mathrm{add}} = 2C_{\mathrm{tr}}k_p$).

NUMERICAL SOLUTION

To convert the evolution equations into a set of coupled ordinary differential equations for each particle size, the population balance equations were discretized with respect to radius $r(i)$. Computationally, discretizing the PBE equations by radius is efficient, since the particle radius increases much more slowly than the particle volume. A number of discrete groups of particles "G" was used in our model, in which each group has a constant radius and one ordinary differential equation describes the particle population in that group. Discritization allows the integro-differential components of the equations to be expressed as finite difference approximations in equally spaced radial increments (Δr). In this work, the backward finite difference approximation was used for deriving the discretized equations.

EXPERIMENTAL SECTION

Materials

The RAFT agent (*o*-ethylxanthyl ethyl propionate) was synthesized in our laboratory according to established procedures.[20] Potassium ethyl xanthogenate (Fluka) of 101.4 g was added to a mixture of 102 g ethyl 2-bromopropionate (Aldrich) dissolved in 1 L of ethanol at 0°C under a nitrogen atmosphere. The mixture was immersed in ice bath and stirred for 6 h in the absence of light. One litre of water was added, and the product was extracted by a 1 : 2 mixture of diethyl ether and pentane.

Milli-Q-standard water was used, and dissolved oxygen was removed by bubbling high purity nitrogen through the mixture of the RAFT agent and monomer for one hour. Styrene monomer, initiator (potassium persulfate), purification columns, and the surfactant (sodium dodecyl sulfate) were obtained from Sigma-Aldrich. Styrene was purified by passing through an inhibitor-removal column. The purification was repeated twice to ensure high purity. All other chemicals were used as received.

RAFT-semibatch emulsion polymerization

Ab initio semibatch emulsion polymerizations were carried out under slight nitrogen pressure in a 1L laboratory reactor equipped with a magnetically driven agitator with a pitched blade impeller operated at 300 rpm. Experiments were conducted with 520 g water, 17.8 g styrene ($M_o = 0.17$ mol), 0.377 g RAFT agent ($AR_o = 0.0017$ mol) with varying amounts of initiator and surfactant at 70 and 80°C. The remaining monomer was added to the reactor via a metering pump at variable flow rates. A temperature controlled circulator (Julabo) provided heating/cooling flows through the external reactor jacket to maintain reaction temperatures at desired levels. The preheated solution of initiator and buffer in water (at the reaction temperature) was added to trigger the reaction. In the first stage, all RAFT agent with surfactant (SDS) and water soluble initiator (KPS), in the presence of monomer (22%), was polymerized for 90 min (batch preperiod), under a slight nitrogen pressure. Thereafter, the monomer was fed continuously into the reactor. Samples were taken periodically to monitor conversion, MWD and PSD. Our procedural details are given in Table I.

Analytical techniques

Monomer conversion was determined gravimetrically off-line with samples from the reactor. The dried polymer was dissolved in tetrahydrofuran (THF, Fluka) to a concentration of 1 m*M*. Analyses were carried out using a high temperature chromatography system (PL-GPC 120) with a PLgel guard 5 μm 50 × 7.5 mm column connected in series with two PLgel (Mixed-C 10 μm 300 × 7.5 mm) columns (PL, Polymer Laboratories) at 40°C. THF was used as eluent at a flow rate of 1 ml/min. Calibration was done using narrow-distribution polystyrene standards (with molecular weights 580 to 7.1 × 10^6 g/mol).A PL Data stream unit was used for data acquisition and the data were processed using Cirrus™ GPC software. The PSD and average particle size were measured using Polymer Laboratory Particle Size Distribution Analysis (PL-PSDA Model

TABLE I
RAFT-Semibatch Emulsion Polymerization Procedures

Run No.	Water (g)	M_o (g)	AR_o (g)	SDS (g)	KPS (g)	F_M (g/min)	F_{AR} (g/min)	T (°C)
Run 1	520	17.8	0.00	1	0.20	0.350	0.00	70
Run 2	520	17.8	0.377	1	0.20	0.00	0.00	70
Run 3	520	17.8	0.377	1	0.20	0.350	0.00	70
Run 4	520	17.8	0.377	1	0.20	0.167	0.00	70
Run 5	520	17.8	0.377	1	0.20	0.531	0.00	70
Run 6	520	17.8	0.377	1	0.35	0.531	0.00	70
Run 7	520	17.8	0.377	1	0.50	0.531	0.00	70
Run 8	520	17.8	0.377	1	0.50	0.531	0.0112	70
Run 9	520	17.8	0.377	2	0.20	0.350	0.00	70
Run 10	520	17.8	0.377	3	0.20	0.350	0.00	70
Run 11	520	17.8	0.377	1	0.20	0.350	0.00	80
Run 12	520	17.8	0.00	1	0.20	0.00	0.00	70

PL-DG2). It uses the principle of packed column hydrodynamic chromatography (HDC) to separate particles in the interstitial void space created by the solid spherical column packing material. The particles eluting from the column are detected using an UV detector.

RESULTS AND DISCUSSIONS

Effect of reaction conditions on monomer conversion

Monomer conversion, defined as the mass ratio of polymer produced to the total amount of monomer added (till time t), is a key factor in determining product properties. Monomer conversion was estimated based on gravimetric measurement of sample solid content. In the model, monomer and AR conversions were calculated from:

$$x_{\text{mon}} = 1 - \frac{N_m}{N_{m,\text{total}}} \tag{46}$$

$$x_{\text{AR}} = 1 - \frac{N_{\text{AR}}}{N_{\text{AR,total}}} \tag{47}$$

where $N_{m,\text{total}}$, $N_{\text{AR,total}}$ are the total amount of monomer and RAFT agent fed into the reactor. Under batch conditions, the total amount of monomer and RAFT are equal to the initially charged amounts ($N_{m,\text{total}} = N_{\text{mo}}$, $N_{\text{AR,total}} = N_{\text{ARo}}$).

Model predictions were compared with experiments for semibatch emulsion polymerization. Figure 1 illustrates monomer conversion as a function of time at variable monomer feed rates [Fig. 1(A)]; whereas Figure 1(B) presents the impact of feeding RAFT agent along with the monomer. In the absence of AR, a high monomer conversion (about 91%) was achieved (Run 1) at the end of the batch preperiod. At this stage, the total amount of monomer available for polymerization in the system is low [Fig. 2(A)]. Hence polymer volume fraction is high ($\Phi_P = 1 - (C_P M_w^M / d_m)$) resulting in glassy particles; under these conditions secondary nucleation is expected unless the free surfactant

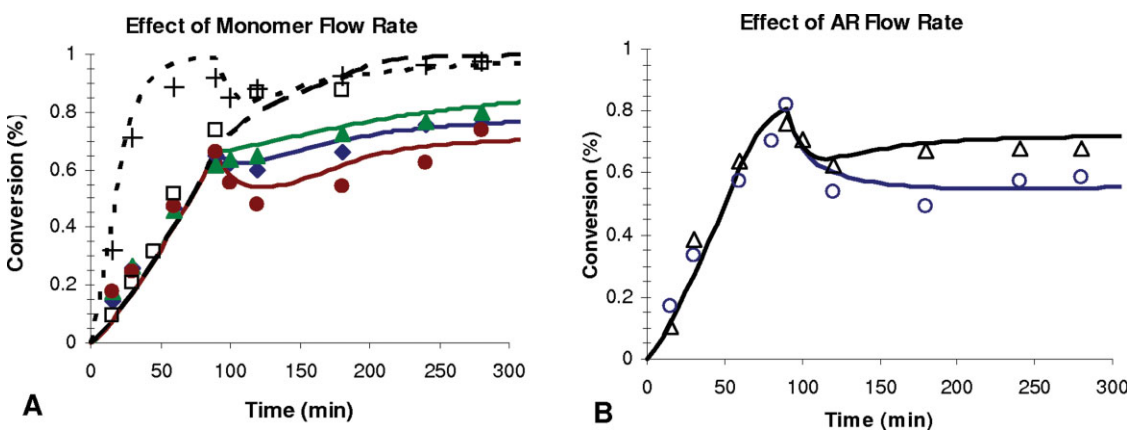

Figure 1 (A) Effect of monomer flow rate (F_M) on the overall monomer conversion for polymerization at 70°C; and, (B) Effect of RAFT agent flow rate (F_{AR}) on monomer conversion. Legend: Run 1 (+); Run 2 (□); Run 3 (▲); Run 4 (◆); Run 5 (●); Run 7 (Δ); Run 8 (○); and model simulations (dashed, dotted, and continuous lines). [Color figure can be viewed in the online issue, which is available at www.interscience.wiley.com.]

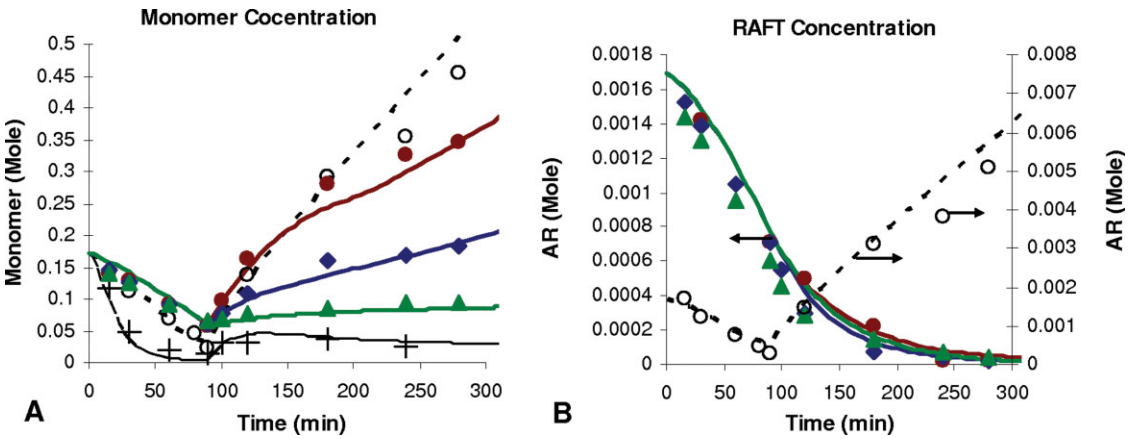

Figure 2 (A) Total number of monomer moles in the reaction vessel; and, (B) Total number of RAFT agent moles in the reaction vessel. Legend: Run 3 (▲); Run 4 (◆); Run 5 (●); Run 8 (○); and model simulations (dotted and continuous lines). [Color figure can be viewed in the online issue, which is available at www.interscience.wiley.com.]

concentration is higher than cmc. The model parameters are given in Table II.

Shortly after the initiating monomer feed, a sudden decrease in monomer conversion was observed. The sudden drop in monomer conversion is due to the accumulation of monomer in the system [Fig. 2(A)] which results in an increase in monomer concentration inside the particles. Compared with the control experiment (Run 1), introducing AR during the batch preperiod resulted in a dramatic decrease in polymerization rate as shown in Figure 1(A) (Runs 2, 3, 4 and 5). In the batch experiment (Run 2, Fig. 1A), as monomer feed rate (F_M) is zero, monomer conversion continues to increase until it approaches that for the control experiment.

The observed retardation indicates that a significant amount of small radicals (R^*) generated by chain transfer were unable to reinitiate polymerization. The ability of such small radicals to reinitiate polymerization inside particles depends mainly on the time they reside in the particles. Thus, the observed retardation is due to the exit of small radicals from particles resulting in reduction in average number of radicals per particle. In the presence of AR, a significant impact of feeding more monomer on the polymerization rate was observed (Runs 3, 4, and 5 in Fig. 1A) in which the final monomer conversions are lower than for batch operation. The observed retardation during the batch preperiod is mainly due to the exit of small radicals formed by exchange with AR and by transfer to monomer.

As the conversion reduction is proportional to monomer flow rate, the effect is due to monomer accumulation in the system. At the beginning of the monomer feed period, AR concentration is low and since F_{AR} is zero, the concentration of AR continues to decrease [Fig. 2(B)] resulting in low concentration of the small radicals produced (R^*). Thus, the differences in monomer conversions between the batch and semibatch runs is mainly due to monomer feed

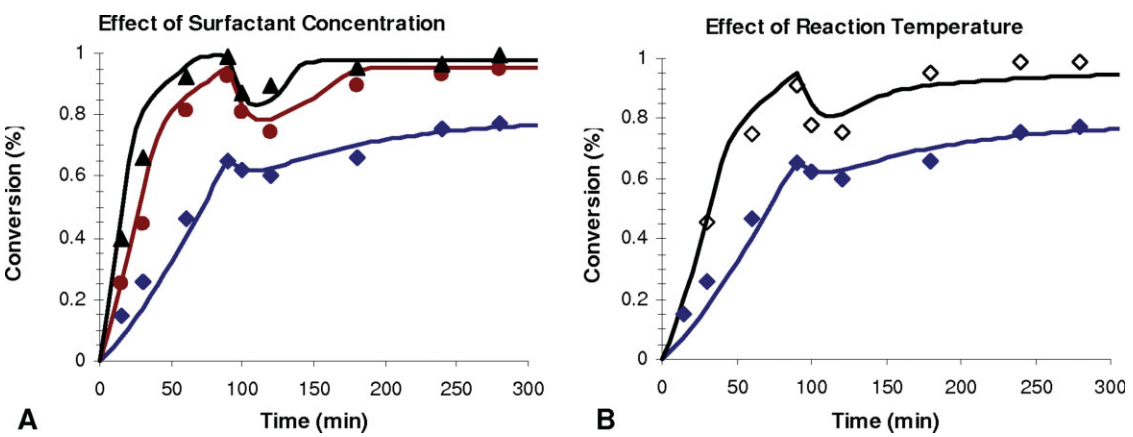

Figure 3 (A) Effect of surfactant concentration on the overall monomer conversion for polymerization at 70°C; and, (B) Effect of reaction temperature on monomer conversion. Legend: Run 4 (◆); Run 9 (●); Run 10 (▲); Run 11 (◊); and model simulations (continuous lines). [Color figure can be viewed in the online issue, which is available at www.interscience.wiley.com.]

TABLE II
List of Parameters Used for Simulating RAFT-Styrene Emulsion Polymerization

Parameter	Value	Ref.	Parameter	Value	Ref.
a_s	42×10^{-18}	6	$k_{\text{frag}}^{\text{RAP}}$	$0.6 \times k_{\text{frag}}$	This work
C_{tr}	1.414exp(−1870/RT)	36, 42	$k_{-\text{frag}}^{\text{RAP}}$	$0.4 \times k_{\text{frag}}$	This work
cmc	0.003	6	$k_{\text{frag}}^{\text{RAR}}$	$k_{-\text{frag}}^{\text{RAP}} = k_{\text{frag}}^{\text{PAP}}$	Assumed
$C_{w\_sat}^{\text{AR}}$	0.002 at 50 °C	36	$k_{\text{frag}}^{\text{PAR}}$	$0.4 \times k_{\text{frag}}$	This work
$C_{p\_sat}^{M}$	5.5	6	$k_{-\text{frag}}^{\text{PAR}}$	$0.6 \times k_{\text{frag}}$	This work
$C_{w\_sat}^{M}$	$e^{(-1.514-1259/T)}$	6	K_{wp}^{M}	$C_{w\_sat}^{M}/C_{p\_sat}^{M}$	7
d_p	1050.1–0.621T	6	$K_{\text{wp}}^{\text{AR}}$	K_{wp}^{M}	Assumed
d_m	923.6–0.887T	7	k_{add}	$2k_pC_{\text{cr}}$	36,43
d_{RAFT}	1.12	This work	$k_{p,\text{aq}}^{1}$	$4k_p$	6,29
D_w	1.55×10^{-7}	6	$K_{p,\text{aq}}^{2}$	$2k_p$	7
j_{crit}	5	6, 30	$k_{p,\text{aq}}^{3}$	k_p	7
k_{tr}	$k_p10^{-0.658}e^{(-23400/\text{RT})}$	6	$k_{p,\text{aq}}^{4}$	$k_{p,\text{aq}}^{3}$	7
$k_{t,\text{aq}} = k_{\text{to}}$	6.8×10^{7}	6, 7	k_p^R	$4k_p$	
k_{po}	$1.259 \times 10^{7}e^{(-29000/\text{RT})}$	6, 7	n_{agg}	60	
k_d	$8 \times 10^{15}\ e^{(-13500/\text{RT})}$	6, 7	z	3	6,30
k_{frag}	$>10^4$	This work	σ	6.02×10^{-9}	7
$k_{\text{frag}}^{\text{PAP}}$	$0.5 \times k_{\text{frag}}$	This work	α	7.4×10^{-9}	7
$k_{-\text{frag}}^{\text{PAP}}$	$k_{\text{frag}}^{\text{PAP}}$	Assumed			

(monomer accumulation) with exit of small radicals having a small effect on reduced monomer conversion during the feed period. This conclusion is further supported by the simulation and experimental results presented in Figure 1(B), where the difference between run 7 and run 8 is that in run 7, F_{AR} was zero and in run 8, F_{AR} was equal to $F_{\text{M}}/100$. Figure 1(B) shows the effect of adding AR (Run 8) along with monomer ($F_{\text{M}}/F_{\text{AR}} = N_{\text{Mo}}/N_{\text{ARo}} = 100$, where F_{M} and F_{AR} are monomer and RAFT agent flow rates, respectively.

For run 7, monomer conversion drops on initiating monomer feed, from 83 to 61% and then increases to about 75% at the end of polymerization. On the other hand, monomer conversion in run 8 drops from 86 to 56% and then continues to decrease to 51% after which monomer conversion levels off at 61%. Due to RAFT feed, the total amount of AR increased (Run 8, Fig. 2B), resulting in production of greater number of small radicals (R*) capable of exiting from the particles and hence inducing further reduction in polymerization rate. Thus, the drop in monomer conversion in runs 3, 4, 5, and 7 is mainly due to monomer accumulation in the system with radical exit having a minor effect; whereas the decrease in monomer conversion in run 8 is due to both monomer accumulation and radical exit.

The amount of surfactant (SDS) was varied to investigate the effect of emulsifier concentration on polymerization rate, MWD and PSD. Figure 3(A) shows the effect of increased surfactant concentration at constant initiator (0.2 g), RAFT (0.375 g), monomer flow ($F_{\text{M}} = 3.37 \times 10^{-3}$ mol/min) and reaction temperature (70°C). As expected, monomer conversion increased with increase in surfactant concentration. Since micellar nucleation is the prevailing mechanism for particle formation, the number of polymeric particles is strongly dependent on surfactant concentration. Consequently, increasing surfactant concentration resulted in increasing the total number of polymerization loci, leading to an increase in polymerization rate. As expected, the polymerization rate was markedly improved by increasing the reaction temperature [Fig. 3(B)]. This is because of the increased number of particles and an increase in the propagation rate.

Effect of reaction conditions on molecular weight

The evolution of MWD records the kinetic events that control polymer formation during polymerization. The Mueller equations, obtained via the method of moments, were used to predict the number average (M_n) and weight average molecular weight (M_w) of the polymer produced by RAFT process. M_n is given by:

$$\overline{M}_n = M_w^{\text{AR}} + \frac{M_o \times x_{\text{mon}}}{\text{AR}_o(1-(1-\alpha)(1-x_{\text{AR}})) + 2f(I_o - I)M_w^M} \quad (48)$$

where M_o, AR_o, and I_o are the initial amounts of monomer RAFT agent and initiator in moles, respectively; I is the undecomposed amount of initiator in

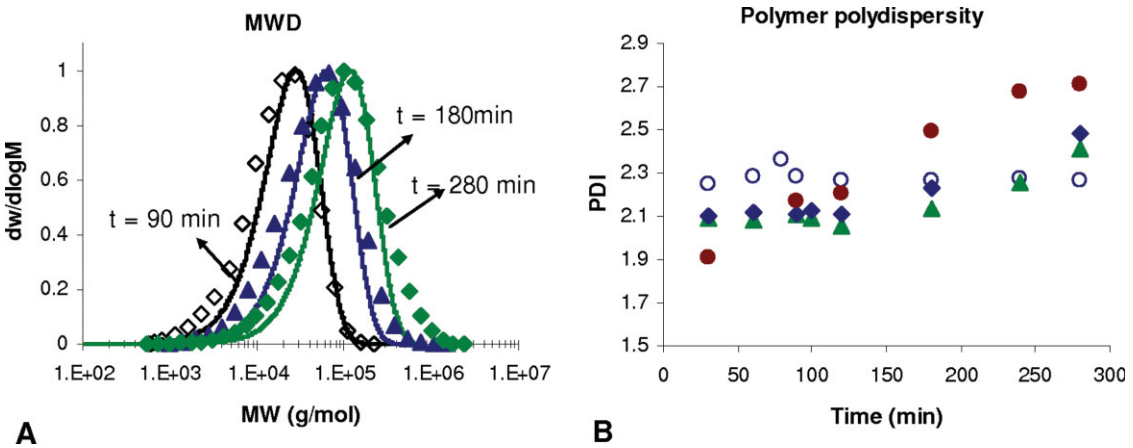

Figure 4 (A) Experimental MWD and molar chain extension with semi-batch emulsion polymerization of styrene with monomer flow rate = 0.531 g/min (Run 7). (B) Polymer polydispersity obtained from runs 3, 4, 5, and 8 at 70°C and variable monomer flow rates. Legend: Run 3 (▲); Run 4 (◆); Run 5 (●); Run 8 (○); and model simulations (continuous lines). Symbols in (A) represent the exprimental MWD at different times. [Color figure can be viewed in the online issue, which is available at www.interscience.wiley.com.]

mole; M_w^M and M_w^{AR} are monomer and AR molecular weights, respectively; x_{AR} is the RAFT agent conversion which is equal to $x_{mon}^{1/C_{tr}}$ in the batch experiment. The instantaneous M_n is approximated by the rate of propagation over the rate of chain stoppage events:

$$\overline{M}_n = \left[\frac{k_p C_p^M}{k_{tr}^{AR} C_p^{AR} + k_{tr}^M C_p^M + \rho_{avg}}\right] \quad (49)$$

These equations are valid for the three intervals if the transport rate of AR from droplets to the particles is equal to or higher than its consumption rate[8] that is, the mass transfer resistance to AR is negligible. For control of M_n, using a xanthate RAFT agent, most of the accumulated polymer is produced by the transfer reaction to the AR; thus, the global AR concentration significantly affects the polymerization rate.[8] Hence, the instantaneously produced polymer presents a Schulz-Flory MWD with a polydispersity index equal to $(1 + 1/C_{tr})$ [Fig. 4(A)] and M_n is given by eq. (48). The chromatograms of run 7 were compared (see Fig. 4A) with simulated chromatograms based on Schulz-Flory distributions estimated from predicted M_n; a good agreement was obtained. Therefore, with an effective molecular weight control, the final MWD follows the Schulz-Flory theory. Figure 4(B) shows that higher monomer feed rate results in higher polydispersities. This is because at higher monomer feed rates, monomer droplets are present in the aqueous phase and monomer concentration is relatively high, resulting in the propagating chain adding large number of monomer units before radical activity transfer. Additionally, the relatively high monomer concentration enhances the occurrence of side reactions and termination in the aqueous phase. These lead to the formation of low molecular weight species and broadening of the MWD.

For batch polymerization with AR ($C_{tr} = 1$), the ratio of the consumption rates of monomer to AR remains constant throughout the reaction, and hence Mn is also constant. In this work, Mn shows a slight decrease with time [Run 2, Fig. 5(A)] indicating that the transfer constant of the AR used in this work is lower than 1. As shown in Figure 5(B) an almost constant Mn can be still obtained if the reaction is carried out under a starved addition of monomer-AR mixture with a molar feed rate ratio during the feeding stage equal to the initial molar ratio of monomer to AR during the batch pre-stage ($F_M/F_{AR} = N_{Mo}/N_{ARo}$). The Mn values, obtained from (Run 8) where AR was fed along with monomer into the reactor, are close to those obtained from the batch experiment (Run 2).

In conventional emulsion polymerization without a transfer agent, M_n is unaffected by changes in monomer flow rate.[7] An increase in temperature results in decreased M_n due to an increase in initiation, transfer to monomer and termination rates relative to the propagation rate. In the presence of AR, the impact of monomer flow rate on M_n is illustrated in Figure 5(A). Runs 3, 4, and 5 were designed to address the effect of increasing monomer flow rate on monomer conversion (Fig. 1), number average molecular weight Mn (Fig. 5) and PSD (Fig. 7). The M_n values are close to each other during the batch prestage and show a slight decrease with time. For the batch experiment [Run 2, Fig. 5(A)], all monomer, AR, surfactant and initiator were loaded into the reactor at the beginning of the polymerization. Thus, Monomer to AR molar ratio was constant, and hence Mn evolution followed a

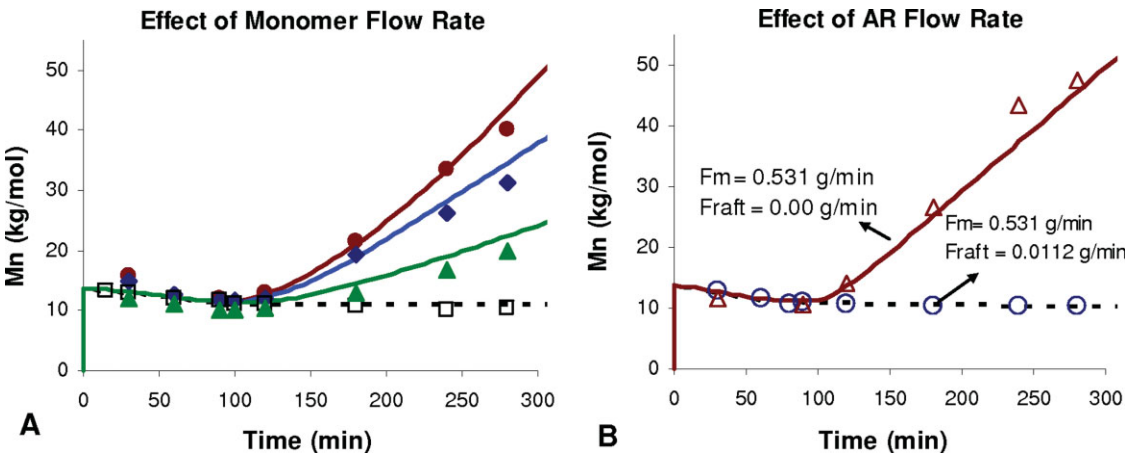

Figure 5 (A) Effect of monomer flow rate (F_M) on the number average molecular weight for polymerization at 70°C; and, (B) Effect of RAFT agent flow rate (F_{AR}) on the number average molecular weight. Legend: Run 2 (□); Run 3 (▲); Run 4 (◆); Run 5 (●); Run 7 (Δ); Run 8 (○); and model simulations (dotted and continuous lines). [Color figure can be viewed in the online issue, which is available at www.interscience.wiley.com.]

continuously decreasing trend. The latexes produced from the batch preperiod were used as the seeds and styrene was slowly added to the reactor during the second stage. During monomer feed at the second stage, M_n increased with time due to the increase in monomer-AR molar ratio in the particle; higher the flow rate higher was observed increase in M_n. That is, the amount of RAFT end-capped polymeric chains remained almost constant, whereas the amount of reacted monomer increased. Increasing SDS from 1 g to 2 g resulted in significant increases in M_n, and with further increase to 3g, resulted in negligible changes in Mn, indicating that the increase in Mn is proportional to monomer conversion [Fig. 6(A)].

As shown by Gugliotta et al.,[1] AR accumulates when it does not attain thermodynamic equilibrium as quickly as the monomer, and the molar ratio of monomer to AR in particles becomes greater than its initial value. This results in an increase in Mn which eventually levels off. In this work, Mn values in run 8 are almost constant. Thus, we conclude that the transport rate of AR from the aqueous phase to the particles is fast enough with negligible mass-transfer resistance to enable rapid thermodynamic partitioning and to maintain the initial molar ratio of monomer to AR at the same level during the reaction. Based on this, the constant partitioning coefficient model used in this work to calculate AR concentration is valid.

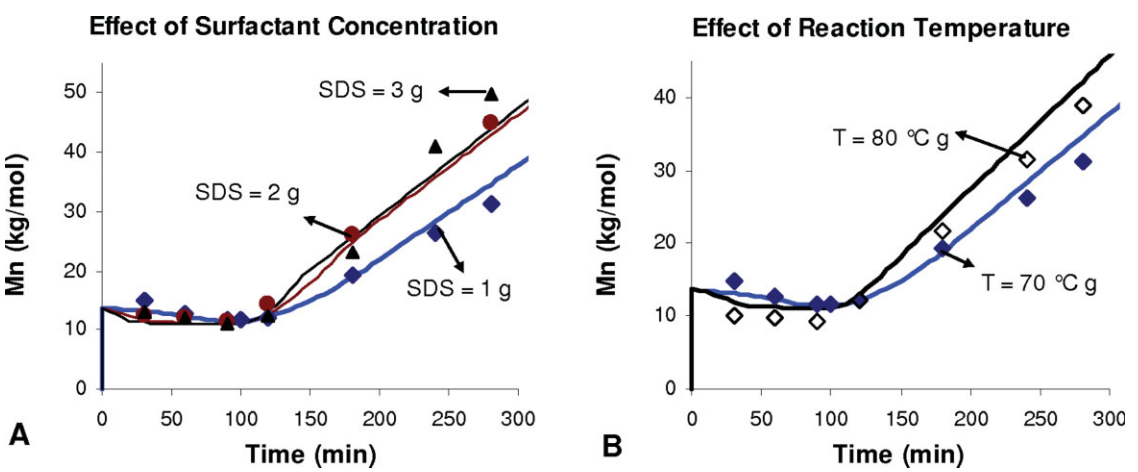

Figure 6 (A) Effect of surfactant concentration on the number average molecular weight for polymerization at 70°C; and, (B) Effect of reaction temperature on the number average molecular weight. Legend: Run 4 (◆); Run 9 (●); Run 10 (▲); Run 11 (◊); and model simulations (continuous lines). [Color figure can be viewed in the online issue, which is available at www.interscience.wiley.com.]

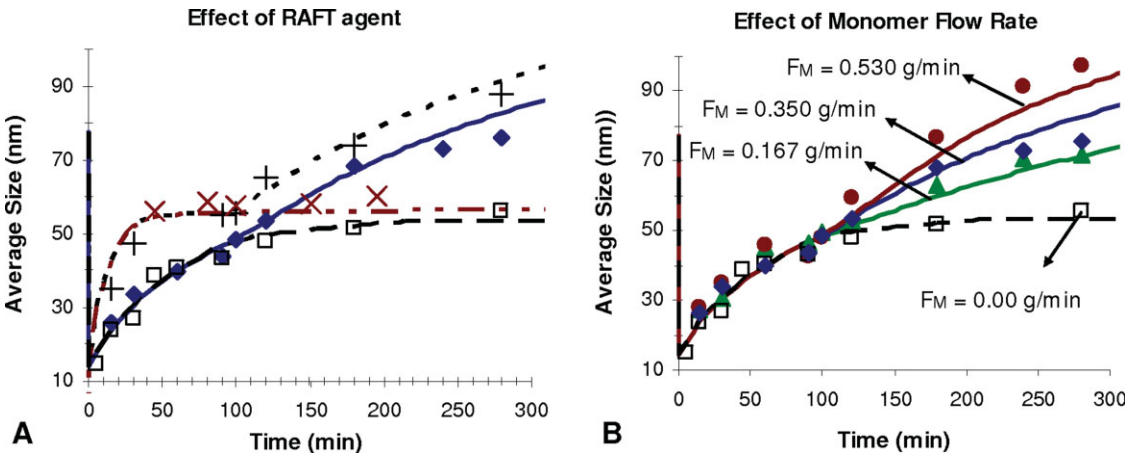

Figure 7 (A) Effect of AR on average particle size (PS) in batch and semi-batch emulsion polymerization at 70°C; and, (B) Effect of variable monomer feed rates on (PS) Legend: Run 1 (+); Run 2 (□); Run 3 (▲); Run 4 (◆); Run 5 (●); Run 12 (×); and model simulations (dashed, dotted, and continuous lines). [Color figure can be viewed in the online issue, which is available at www. interscience.wiley.com.]

The effect of surfactant concentration and reaction temperature on Mn is shown in Figure 6(A,B), respectively. As the temperature was increased from 70 to 80°C, Mn decreased during the batch stage and increased during the monomer feed stage. Thus, Mn is controlled by the relative rates of propagation and chain transfer. Under similar monomer flow rates, the increase in Mn during monomer feed stage at the higher temperature is due to increases in propagation rate resulting in greater monomer conversion. During the batch stage, the increased number of chains due to increased transfer reaction rate resulted in decrease in Mn. Due to its low transfer coefficient, the evolution of Mn (Fig. 5A, Run 2 and Figure 5(B), Run 8) remains almost constant over the period of polymerization with no linear growth. This may lead one to surmise that xanthates act as conventional irreversible chain transfer agents and are not able to induce living characteristics. In contrast, experimental data from semibatch styrene emulsion polymerization with o-ethylxanthyl ethyl propionate (Runs 3, 4, and 5 in Figure 5(A). Run 7 in Figure 5(B) and Runs 9, 10, 11 in Figure 6(A,B)) indicate that a high proportion of the previously prepared polystyrene-xanthate chains (at the batch stage) act as macro-RAFT agents which enable chain extension when a subsequent batch of monomer is added.

Thus, the chain extension confirms that the previously prepared polymeric chains were able to regain radical activity and hence demonstrate the living nature of the polymer in the presence of xanthates. In case the previously prepared chains did not possess the living nature, the newly added monomers would have polymerized separately, resulting in high and uncontrolled polydispersity or increase in MWD modality. The unimodal MWD for the extended polystyrene-xanthate chains (Fig. 4A, run 7) confirms that previously prepared polystyrene-xanthate chains were involved at the second stage with newly added monomer. In terms of MWD, feeding AR along with monomer shows no difference in comparison with the batch experiment. Therefore, MWD control requires only intermediate monomer addition, or the independent and simultaneous addition of monomer and AR.

Effect of reaction conditions on particle size

In estimating the particle size distribution, we accounted for the swollen and unswollen (absence of monomer) particle sizes. The swollen (r_S) and unswollen (r) radiuses are related by mass conversion (assuming ideal mixing of monomer and polymer) as follows:

$$\frac{r_s}{r} = \left[\frac{d_m}{d_m - C_p^M M_0}\right]^{1/3} \tag{50}$$

where d_M is the density of monomer.

The predicted and experimentally measured particle sizes show dramatic decrease with increasing RAFT agent from 0.00 g [Run 12 in Figure 7(A), batch experiment without RAFT] to 0.375 g [Run 2 in Figure 7(A), batch experiment with RAFT]. To investigate the effects of interim monomer addition, both runs 2 and 12 were repeated, and the results for semibatch operation are shown in Figure 7(A) (Run 1 without RAFT and Run 4 with RAFT).

During the batch preperiod, experimental conditions are similar to those for batch experiments; hence, the measured particle sizes are close to each other. In the batch experiment without AR (Run 12), the growth rate of particle is higher due to the absence of rate retardation. Once all monomers have

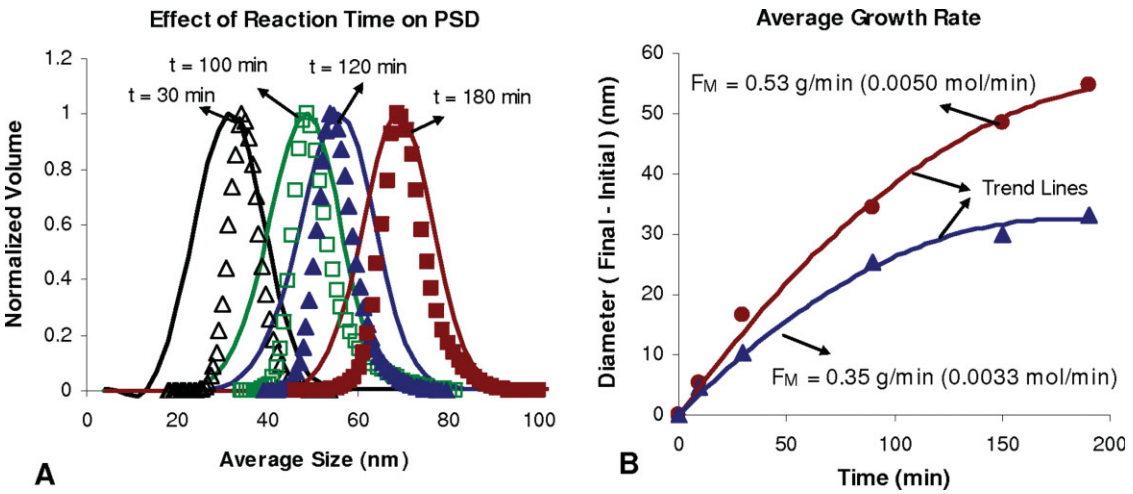

Figure 8 (A) Experimental and simulated PSD at moderate monomer feed rate (Run 4), samples were taken at different reaction times; and (B) Experimental average growth rate of the polymer particles at different monomer feed rates. Legend: Run 4 (◆); Run 5 (●); and model simulations (continuous lines). Symbols in (A) represent the experimental PSD at different times. [Color figure can be viewed in the online issue, which is available at www.interscience.wiley.com.]

reacted, the maximum value of particle size is attained in a short period (50 min), after which it levels off. For the batch experiment with AR (Run 2), particle size increases slowly due to the effect of rate retardation. Thus, it takes significantly longer (280 min) to attain the same size as in run 12. An increase in particle size was observed immediately after the initiation of monomer feed in both semi-batch experiments with and without AR, run 4 and run 1, respectively.

As shown in Figure 7(B), variable particle sizes were obtained using the same recipe but with different monomer feed rates. Equation (14) shows that particle growth is strongly affected by monomer concentration. At high feed rate, the process resembles interval II as seen in the batch run (i.e., the presence of monomer droplets in aqueous phase). Monomer concentration inside polymer particles increases with an increase in feed rate, eventually reaching saturation. Equation (14) indicates that particle growth rate, which depends strongly on monomer concentration, is relatively high under these conditions. Consequently, polymer volume fraction [eq. (19)] inside the particles is less than 0.8 (typically ~ 0.46) and larger particles are obtained. As the reaction progresses, monomer concentration inside the particles becomes less than its saturation value (<5.5 *M*) resulting in Φ_P exceeding the limiting value of 0.80. Thereby, the particles become glassy and the system enters a diffusion controlled regime, resulting in the suppression of propagation rate and particle growth. This is observed with runs 3 and 4 [Fig. 7(B)], where monomer feed rates are lower and monomer conversions are higher compared with run 5.

Figure 8(B) shows the relation between monomer flow rate and average growth rate of particles. During the batch preperiod, the experimental conditions for runs 3, 4, and 5 are similar, resulting in almost similar average growth rates of particles and hence all particle sizes during this period are almost similar. In Figure 8(B), the initial particle size (PS) was taken to be the one at the end of the batch preperiod so as to address the impact of monomer addition on PSD. It was observed that increasing monomer feed rate resulted in a larger particle growth rate (Run 5, Fig. 8B). For a lower monomer feed rate (Run 4, Fig. 8B), the particle growth rate is lower and approaches a steady state after 150 min of monomer feeding.

In conclusion, higher the monomer feed rate, larger the particle size and slower the particle growth rate, which approaches a steady state. At constant surfactant concentration, the particle size is roughly proportional to monomer conversion in runs 2, 3, 4, and 5. Thus, the retardation in particle growth rate compared with RAFT-free experiments (Runs 1 and 12) is most likely due to radical exit. As the concentration of AR and hence that of the AR radicals increases, these radicals exit from the particles resulting in ceasing of particle growth; thus, reducing the average particle size.

As shown in Figure 8(A), PSD obtained from run 4 (moderate monomer feed rate) at different reaction times are narrow and the PSD for each sample is represented by one Gaussian peak, indicating the absence of secondary or homogeneous nucleation. Propagation of the aqueous phase radical to j_{crit} degree occurs with particles swollen with monomer. The absence of secondary nucleation indicates that homogeneous polymerization to j_{crit} degree is insignificant and almost all of the aqueous phase radicals (exited and initiator derived radicals) are efficiently captured by the pre-existing particles (particles

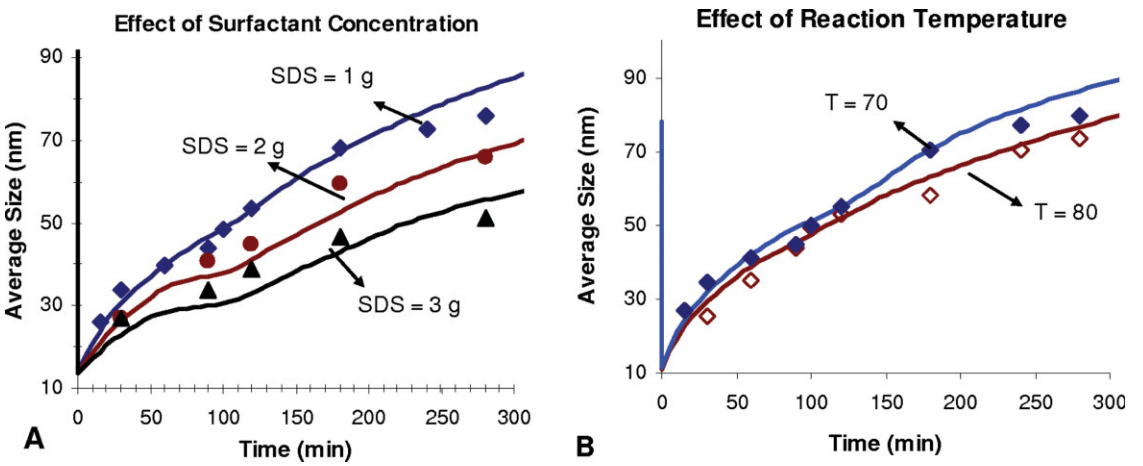

Figure 9 (A) Effect of SDS concentration on the average particle size (PS) in batch and semi-batch emulsion polymerization at 70°C; and, (B) Effect of reaction temperature on (PS) Legend: Run 4 (◆); Run 9 (●); Run 10 (▲); Run 13 (◊); and model simulations (continuous lines). [Color figure can be viewed in the online issue, which is available at www.interscience.wiley.com.]

formed via micellar nucleation). Surfactant plays a crucial role in the nucleation process and on the number of particles formed. Runs 4, 9, and 10, were designed to investigate the effect of surfactant on monomer conversion, MWD and PSD. The final average particle size decreases as SDS concentration increases [Fig. 9(A)]. We note that the concentration of initiator and AR in runs 4, 9, and 10 are similar, and the changes in the PSDs are entirely due to changes in SDS concentration. A high surfactant concentration results in a large number of particles, and a small number of radicals per particle.

Thus, with an increased SDS, each particle receives smaller number of radicals resulting in a particle with a low probability to grow in size. During the monomer feed period (reaction time: from 90 to 300 min), the continuous increase in the particle size is due to the monomer addition, which sustains monomer concentration inside the particle. Consequently, the process of particle growth driven by propagation reactions is enhanced. Similarly, Figure 9(B) shows that an increase in reaction temperature results in smaller average particle size due to increase in oligomeric radical concentration in the aqueous phase and increase in nucleation rate. Consequently, the total number of particles increases at the expense of size.

CONCLUSIONS

A mathematical model was developed to describe *ab initio* emulsion polymerization of styrene with *o*-ethylxanthyl ethyl propionate as RAFT agent (AR). The model accounts for the effects of RAFT agent on the polymerization rate, number average molecular weight, weight average molecular weight, molecular weight distribution, polydispersity index, particle average radius, and particle size distribution. The model was validated against experimental data obtained in our laboratory. The reactions were carried out using variable AR agent, surfactant (SDS), and initiator (KPS) at different reaction temperatures. Polymerization rate was found to be retarded by increasing AR concentration. The observed retardation was attributed to small radicals exiting from the polymeric particles.

The decline in conversion, observed to be proportional to monomer flow rate, was due to monomer accumulation in the particles when there is no RAFT feed. Further, monomer conversion was reduced due to the added effect of radical exit when the RAFT agent was fed into the reactor along with the monomer. Increase in surfactant concentration resulted in increase in the total number of polymerization loci, leading to an increase in the polymerization rate. The polymerization rate was markedly improved by increasing the reaction temperature. This is due to an increase in the propagation rate. We investigated the effect of monomer and AR on Mn. During the batch period, Mn values were close to each other because the reaction conditions were similar. During the monomer feed period, Mn increased due to the increase in monomer/AR molar ratio in the particle. When the RAFT agent was fed along with the monomer, no change in Mn was observed, indicating that a rapid thermodynamic partitioning was achieved. The living nature of the process was confirmed by the unimodal MWD for the extended polystyrene-xanthate chains.

Similar to Mn, monomer feed rate was found to have a profound effect on the growth of the particles, as the particle size increased with monomer feed rate. Typical particle size for uncontrolled

radical emulsion polymerization range from 50 to 200 nm. Polymerizations carried out with AR have been shown to provide emulsions with smaller particle size under similar conditions of surfactant and monomer concentrations. These indicate that controlling MWD and PSD is feasible by manipulating the surfactant and RAFT concentrations, reaction temperature and most importantly the interim monomer and AR flow control in semibatch, either independently or simultaneously. Our model accurately predicts the effects of the RAFT agent, surfactant and initiator on the measured polymer properties.

We acknowledge the financial support of the Australian Research Council for this work. Our simulations were carried out using the gPROMS (PSE) software.

References

1. Gugliotta, L. M.; Salazar, A.; Vega, J. R.; Meira, G. R. Polymer 2001, 42, 2719.
2. Mendoza, J.; De La Cal, J. C.; Asua, J. M. J Polym Sci Part A: Polym Chem 2000, 38, 4490.
3. Matyjaszewski, K.; Xia, J. Chem Rev 2001, 101, 2921.
4. Moad, G.; Rizzardo, E.; Thang, S. H. Aust J Chem 2005, 58, 379.
5. Schulte, T.; Knoop, C. A.; Studer, A. J Polym Sci Part A: Polym Chem 2004, 42, 3342.
6. Gilbert, R. G. Emulsion Polymerization: A Mechanistic Approach; 1st ed.; Academic Press: London, 1995; p 362.
7. Zeaiter, J.; Romagnoli, J. A.; Barton, G. W.; Gomes, V. G.; Hawkett, B. S.; Gilbert, R. G. Chem Eng Sci 2002, 57, 2955.
8. Altarawneh, I. S.; Gomes, V. G.; Srour, M. S. Macromol React Eng 2008, 2, 58.
9. Butte, A.; Storti, G.; Morbidelli, M. Macromolecules 2001, 34, 5885.
10. Butte, A.; Storti, G.; Morbidelli, M. Macromolecules 2000, 33, 3485..
11. Hermanson, K. D.; Liu, S.; Kaler, E. W. J Polym Sci Part A: Polym Chem 2006, 44, 6055.
12. Luo, Y.; Cui, X. J Polym Sci Part A: Polym Chem 2006, 44, 2837.
13. Kwak, Y.; Goto, A.; Fukuda, T. Macromolecules 2004, 37, 1219.
14. Monteiro, M. J.; Hodgson, M.; De Brouwer, H. J Polym Sci Part A: Polym Chem 2000, 38, 3864.
15. Chiefari, J.; Chong, Y. K.; Ercole, F.; Krstina, J.; Jeffery, J.; Le, T. P. T.; Mayadunne, R.; Meijs, G. F.; Moad, C. L.; Moad, G.; Rizzardo, E.; Thang, S. H. Macromolecules 1998, 31, 5559.
16. Charmot, D.; Corpart, P.; Adam, H.; Zard, S. Z.; Biadatti, T.; Bouhadir, G. Macromol Symp 2000, 150, 23.
17. Monteiro, M. J.; De Barbeyrac, J. Macromolecules 2001, 34, 4416.
18. Prescott, S. W.; Ballard, M. J.; Rizzardo, E.; Gilbert, R. G. Aust J Chem 2002, 55, 415.
19. Prescott, S. W.; Ballard, M. J.; Rizzardo, E.; Gilbert, R. G. Macromolecules 2002, 35, 5417.
20. Smulders, W. W.; Gilbert, R. G.; Monteiro, M. J. Macromolecules 2003, 36, 4309.
21. Apostolovic, B.; Quattrini, F.; Butte, A.; Storti, G.; Morbidelli, M. Helv Chim Acta 2006, 89, 1641.
22. Ferguson, C. J.; Hughes, R. J.; Nguyen, D.; Pham, B. T. T.; Gilbert, R. G.; Serelis, A. K.; Such, C. H.; Hawkett, B. S. Macromolecules 2005, 38, 2191.
23. Moad, G.; Chiefari, J.; Chong, Y. K.; Krstina, J.; Mayadunne, R. T. A.; Postma, A.; Rizzardo, E.; Thang, S. H. Polym Int 2000, 49, 993.
24. Monteiro, M. J.; Sjoberg, M.; Van Der Vlist, J.; Gottgens, C. M. J Polym Sci Part A: Polym Chem 2000, 38, 4206.
25. Smulders, W. W.; Monteiro, M. J. Macromolecules 2004, 37, 4474.
26. Luo, Y.; Wang, R.; Yang, L.; Yu, B.; Li, B.; Zhu, S. Macromolecules 2006, 39, 1328.
27. Peklak, A. D.; Butte, A. J Polym Sci Part A: Polym Chem 2006, 44, 6114.
28. Prescott, S. W. Macromolecules 2003, 36, 9608.
29. Prescott, S. W.; Ballard, M. J.; Rizzardo, E.; Gilbert, R. G. Macromol Theory Simul 2006, 15, 70.
30. Coen, E. M.; Gilbert, R. G.; Morrison, B. R.; Leube, H.; Peach, S. Polymer 1998, 39, 7099.
31. Altarawneh, I. S.; Srour, M.; Gomes, V. G. Polymer Plast Technol Eng 2007, 46, 1103.
32. Casey, B. S.; Morrison, B. R.; Maxwell, I. A.; Gilbert, R. G.; Napper, D. H. J Polym Sci Part A: Polym Chem 1994, 32, 605.
33. Hawkett, B. S.; Napper, D. H.; Gilbert, R. G. J Chem Soc Faraday Trans 1 1980, 76, 1323.
34. Coen, E. M.; Peach, S.; Morrison, B. R.; Gilbert, R. G. Polymer 2004, 45, 3595.
35. Thickett, S. C.; Gilbert, R. G. Polymer 2007, 48, 6965.
36. Smulders, W. W. Macromolecular architecture in aqueous dispersions: 'living' free-radical polymerization in emulsion; Technische Universiteit Eindhoven: Eindhoven, Netherland 2002; p. 196.
37. Maxwell, I. A.; Morrison, B. R.; Napper, D. H.; Gilbert, R. G. Macromolecules 1991, 24, 1629.
38. Monteiro, M. J.; De Brouwer, H. Macromolecules 2001, 34, 349.p.
39. Gugliotta, L. M.; Arzamendi, G.; Asua, J. M. J Appl Polym Sci 1995, 55, 1017.
40. Salazar, A.; Gugliotta, L. M.; Vega, J. R.; Meira, G. R. Ind Eng Chem Res 1998, 37, 3582.
41. Buback, M.; Gilbert, R. G.; Hutchinson, R. A.; Klumperman, B.; Kuchta, F. D.; Manders, B. G.; O'Driscoll, K. F.; Russell, G. T.; Schweer, J. Macromol Chem Phys 1995, 196, 3267.
42. Adamy, M.; Van Herk, A. M.; Destarac, M.; Monteiro, M. J. Macromolecules 2003, 36, 2293.
43. Moad, G.; Mayadunne, R. T. A.; Rizzardo, E.; Skidmore, M.; Thang, S. H. ACS Symp Ser 2003, 854, 520.